International Journal of Mass Spectrometry 295 (2010) 149–152

Contents lists available at ScienceDirect

International Journal of Mass Spectrometry

journal homepage: www.elsevier.com/locate/ijms

Ion isolation and collision-induced dissociation in a 0.5 mm r_o cylindrical ion trap

A.V. Jesseph, J.D. Fox, G.F. Verbeck IV*

University of North Texas, 1155 Union Circle, 305070, Denton, TX 76203, United States

ARTICLE INFO

Article history:
Received 22 January 2010
Received in revised form 23 March 2010
Accepted 24 March 2010
Available online 31 March 2010

Keywords:
Tandem mass spectrometry
Miniaturization
Cylindrical ion trap

ABSTRACT

We present data taken from a 0.5 mm r_o cylindrical ion trap to track the performance of storage and tandem experiments. The cylindrical ion trap and other mass selecting devices are compared in light of miniaturization. The core components of a cylindrical ion trap mass spectrometer, including ion optics, mass selector assembly, detector, ion source, and housing are described. In these experiments, mass spectral data of xylene is presented. Isolation of the precursor ion was accomplished by modulating the DC ramp voltage, and collision-induced dissociation was accomplished by applying various tickle voltages to the endcaps of the ion trap. Conclusions of projected performance of smaller ion traps (approximately 1 μm) will also be discussed.

1. Introduction

In the past decade, much attention has been given to the miniaturization and ruggedization of analytical instrumentation in the effort to develop field-portable devices for real-time sampling and analysis [1]. Mass spectrometry has been a major area of interest in this recent trend for its potential use in a number of applications ranging from environmental monitoring [2] to chemical weapons detection [3,4]. Miniaturization carries benefits conducive to portability such as reduced power requirements and simplification of the vacuum systems, e.g., via the use of chemical getter pumps. To date, a number of lab groups have had success in developing miniature instruments, including a sub-millimeter cylindrical ion trap (CIT) capable of collision-induced dissociation and MS^n experiments [5], a portable rectilinear ion trap [6], a small toroidal ion trap [7], a coaxial ring ion trap [8] and a miniature time of flight (TOF) mass spectrometer [9].

Two of the greatest concerns in miniaturizing mass analyzers are maintaining resolution and minimizing ion attenuation. The issues with ion attenuation are apparent: as the dimensions of the instrument decrease, space charge and surface charge effects increase, thus decreasing the amount of ions that are either trapped or guided in a given period of time. For quadrupole ion traps, the number of ions that can be trapped ($N_{\max}$) is proportional to the depth of the pseudopotential well (D_z) [10]:

$$N_{\max} = \frac{3D_z}{4\pi e z_0^2}, \tag{1}$$

where e is the elementary electronic charge, z_0 is the field size parameter for the ion trap and:

$$D_z = \frac{eV^2}{4mz_0^2\omega^2}, \tag{2}$$

where e is the elementary electronic charge, V is the zero-to-peak radio frequency (rf) voltage applied to the trap, m is the ionic mass and ω is the angular frequency of the applied field. A variation of these equations can be used to approximate the maximum number of ions stored in cylindrical ions traps [11]:

$$N_{\max} = \frac{3\varepsilon_0 V^2}{4m\omega^2 z_0{}^4} \tag{3}$$

where ε_0 is the permittivity of free space. As the CIT size is reduced the number of ion stored in that trap is reduced. A typical 1.0 cm trap can hold approximately 10^6–10^7 ions and a 1.0 mm trap will hold approximately 10^5 ions. This relationship between trap size and ion attenuation is detrimental to the successful development of small, single miniature ion traps. However, if the number of CITs is increased as the trap radius is reduced, then the total number of ions stored in all traps combined increases. Fig. 1 shows the relationship of ions stored in all traps and number of traps versus trap radius. Assuming that the trap spacing is equal to trap diameter, it can be seen that in a 1.0 cm footprint, 2500 arrayed CITs (at 50 μm r_o) is the beginning of increased ion storage as compared to a single CIT. Fig. 2 is a simple representation of how smaller ion traps can be arrayed on a 1 cm × 1 cm chip. With the arraying of multiple ion traps the perceived problem of signal attenuation inherent in miniaturization is avoided. Trap arraying has recently been explored by several groups [12–16]. Another benefit of reducing CIT size is the potential to run the instrument at higher pressures while maintaining or gaining signal intensity [17].

---

* Corresponding author. Tel.: +1 940 369 8423.
E-mail address: gverbeck@unt.edu (G.F. Verbeck IV).

1387-3806/$ – see front matter © 2010 Elsevier B.V. All rights reserved.
doi:10.1016/j.ijms.2010.03.008

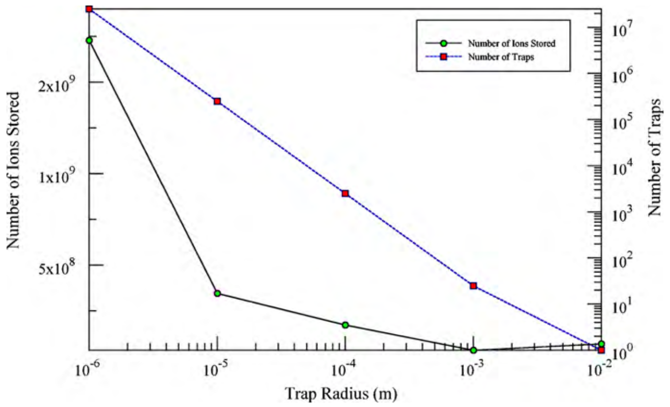

Fig. 1. Number of ions stored and number of traps as a function of trap radius in a CIT array on a 1.0 cm^2 cross section.

To avoid losses in resolution, the use of a cylindrical ion trap (CIT) is natural when miniaturization is in focus. In devices other than the CIT, resolution typically decreases as the device size decreases. The time of flight (Eq. (4)) and linear quad (Eq. (5)) have resolutions both directly dependent on length, while the CIT and quadrupole ion trap (QIT) have resolution dependent on trapping time and resolution can be increased with trapping time at the cost of signal strength (Eq. (6)).

$$\text{TOF} \quad R \propto \frac{L}{E_z} \tag{4}$$

$$\text{LQ} \quad R \propto \frac{1}{E_z}\left(\frac{L}{\pi r}\right)^2 \tag{5}$$

$$\text{QIT} \quad R \propto D_z t \tag{6}$$

It can be seen that the TOF and linear quad are both length dependent and therefore somewhat more difficult to miniaturize than the QIT while retaining resolution. A reflectron [18,19] TOF has been proposed to lengthen the TOF in a more space-efficient manner [20]. The CIT is easier to fabricate than hyperbolic ion traps [21], and as surface defects and abnormalities become increasingly problematic during miniaturization, ease of manufacturing must be considered. Also, when arraying multiple CITs, simple structures such as a cylinder versus a hyperbolic surface are desired for consistency. This geometry can be manufactured with precision using silicone-on-insulator (SOI) deep reactive ion etching (DRIE) [8]. A miniature CIT has the advantage of reduced power and voltage requirements as the trap size is decreased [22]. Currently, the CIT is the most favorable choice for miniaturization due to its independence from the length parameter and potential for expanding analysis via MS^n experiments. This paper will discuss the design and implementation of such and ion trap as well as preliminary data and plans for a self-contained deployable unit.

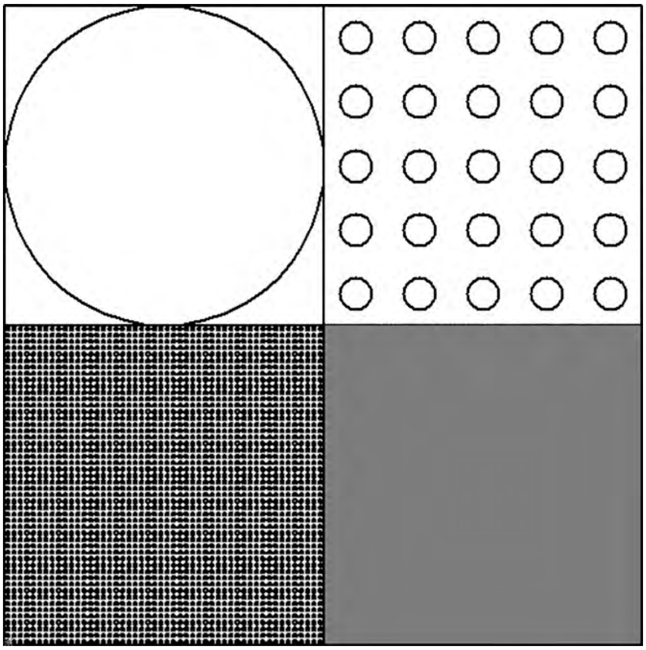

Fig. 2. Four visual representations of ion trap arrays on a 1.0 cm^2 footprint with 0.5 cm, 0.05 cm, 0.005 cm and 0.0005 cm r$_o$.

2. Experimental

A cross section of the instrument can be seen in Fig. 3. The 0.5 mm r$_o$ CIT (V), endcaps (IV) and focusing lenses (III) were machined from stainless steel and housed in a cylindrical casing (I) machined from Vespel® (DuPont, Wilmington, DE). MACOR spacers (Corning Inc., Corning, NY) were used to position the electrodes appropriately and 0.025 mm Kapton film (DuPont, Wilmington, DE) was used to insulate the ion trap from the 0.381 mm endcaps. Ionization was accomplished via an ES-526 yttria-coated iridium disc cathode (II) (Kimball Physics, Wilton, NH). Ion detection was accomplished using a custom channeltron electron multiplier with a gain of 3.3×10^7 (VI) (De Tech Inc., Palmer, MA). The RF voltage and amplitude modulation voltage for the mass-selective instability scan was generated using an arbitrary function generator (Tektronix, Beaverton, OR) and amplified using and AR broadband amplifier (Amplifier Research, Bothell, WA). The assembly was mounted to a 6.99 cm conflat flange and housed in four-way cross (MDC, Hayward, CA). Vacuum was maintained by an MDP turbomolecular pump (Alcatel, Hingham, MA) backed by a DS 302 rotary-vane pump (Varian, Palo Alto, CA), and pressure was monitored using a MicroPirani™ vacuum gauge (MKS, Andover, MA). The typical base pressure for the chamber was approximately

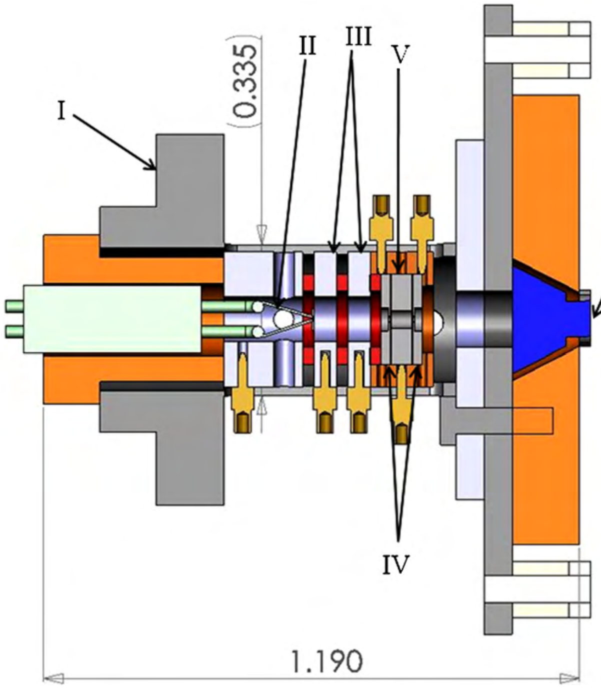

Fig. 3. Cross sectional view of the miniature cylindrical ion trap: (I) Vespel® housing, (II) filament, (III) focusing lenses, (IV) endcaps, (V) trapping ring, (VI) channeltron. Dimensions listed are in inches.

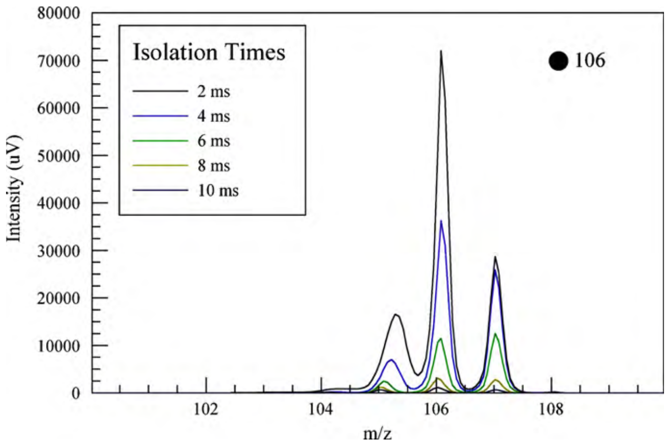

Fig. 4. Mass spectra of xylene product ions (105, 106, 107 *m*/*z*) versus absolute intensity (uV) for isolation times at 2, 4, 6, 8, 10 ms.

10^{-6} Torr. Data was collected using a Tektronix 3034B oscilloscope (Tektronix, Beaverton, OR).

The 0.5 mm r_o ion trap was run at a trapping frequency of 4.3 MHz with an amplitude of 275 V_{0-p} and a 20 Hz repetition rate. During each repetition, the ion source was opened and the trapping frequency was applied to the CIT for approximately 20 ms. Afterwards, the ion source was gated and the detector was brought to its operational voltage prior to and during the ejection sequence. The trap was calibrated using 1.0% SF_6 in helium (not shown), and the common SF_5^+ and SF_3^+ ions. For the initial experiments, the headspace of a liquid xylene sample was introduced to the vacuum chamber via a variable leak valve (MDC, Hayward, CA) until a pressure of approximately 10^{-4} Torr was reached. Tests were performed to probe the isolation efficiency of the trap as a function of time, which was accomplished by modulating the amplitude of the RF voltage to eject ions with mass-to-charge ratios greater and lower than the singly charged xylene ions. Ion ejection during detection was accomplished by increasing the amplitude of the RF voltage in a normal mass-selective instability scan.

After isolation, collision-induced dissociation was accomplished by applying a tickle voltage to the endcaps to increase collision energy and fragmentation by increasing the depth of the potential well in the trap. In the first experiment, the voltage on the endcaps was held at 1 V and the time for CID was varied between 2 and 10 ms. In the second experiment, the isolation time was held constant, 10 ms, while the endcap voltage was varied between 0 and 1 V, in 100 mV increments, in order to examine the effect of CID voltage on ion signal. Data was collected, isolating the 106 *m*/*z* precursor ion and monitoring the range of 88–93 *m*/*z* for the 91 *m*/*z* product ion.

3. Results and discussion

The mass spectra of the isolated xylene ions can be seen in Fig. 4. The molecular ion peak at 106 *m*/*z* is most prominent, followed by the $[M+H]^+$ and $[M-H]^-$ ion peaks at 107 and 105 *m*/*z* respectively. As the isolation time increases, the total ion signal from the trap decreases as more xylene ions are lost during the trapping event (as seen in Fig. 5).

The CID spectra of xylene as a function of collision time can be seen in Fig. 6. Here, the loss of a methyl group from the ring is apparent from the prominent peak at 91 *m*/*z*. Collision time plays a significant role in the retention of ions in the trap. This is evidenced by the large reductions in the integrated signal between 3–4 ms and 4–5 ms (Fig. 7). After 6 ms, the signal is reduced to less than a tenth of its original intensity. The temperature of the product ions becomes significant so that the narrow well of the 0.5 mm r_o ion trap and linear dampening cannot hold an appreciable amount of ions in the trap.

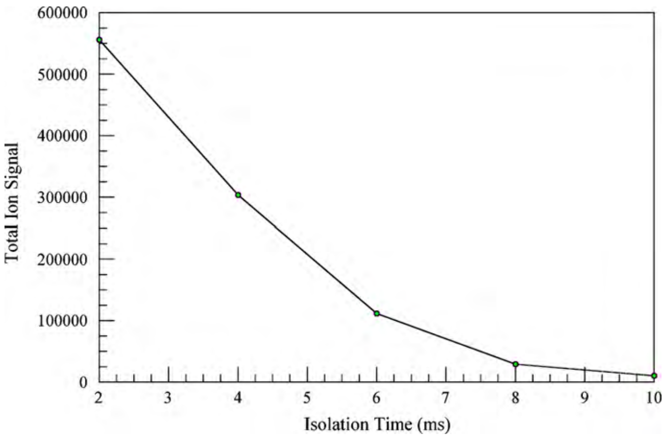

Fig. 5. Integrated ion signals for xylene at different isolation times.

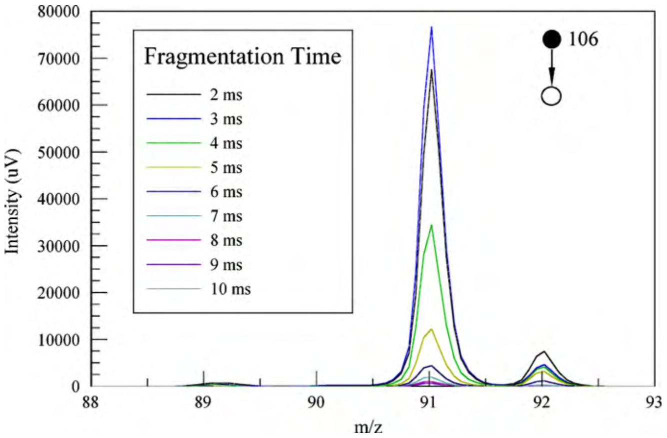

Fig. 6. Mass spectra of xylene product ions (91 and 92 *m*/*z*) versus absolute intensity (uV) for CID times at 2–10 ms at 1 V.

Fig. 8 shows the CID spectra of xylene with different tickle voltages applied to the end caps. No significant signal loss is observed until the endcap voltages exceed 400 mV (Fig. 9). This will increase further product ions, requiring a lower q to see. However, lowering the q will lead to even more ion losses.

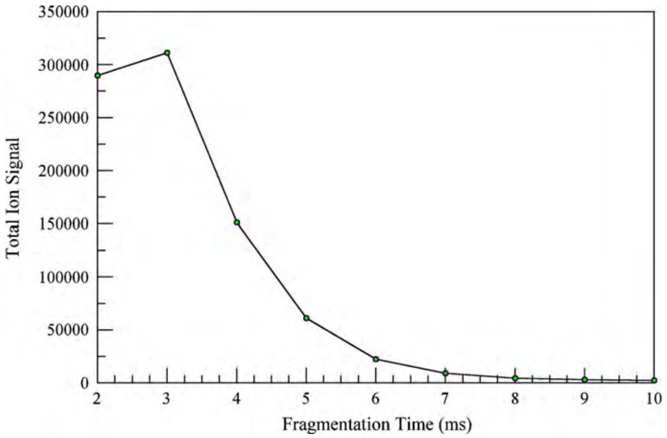

Fig. 7. Integrated signals from the mass spectra of xylene with incrementally longer CID times.

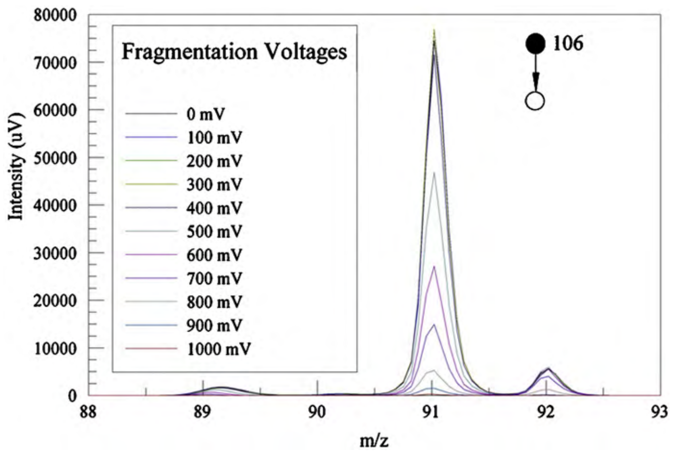

Fig. 8. Mass spectra of xylene product ions (91 and 92 *m*/*z*) versus absolute intensity (uV) at 0–1 V CID energy at 10 ms CID time.

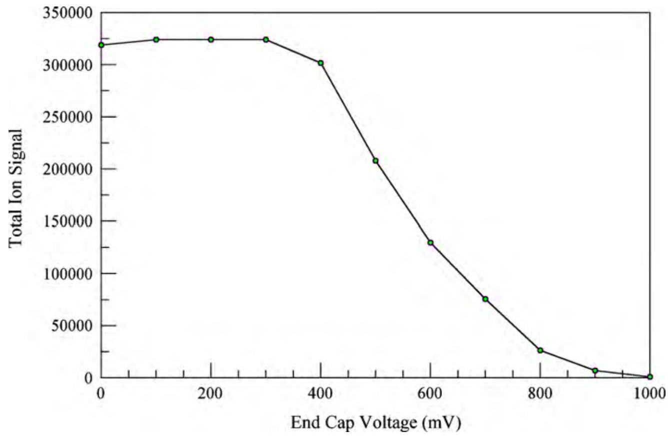

Fig. 9. Integrated signals from the mass spectra of xylene at different CID voltages.

The parameters that affect ion retention during CID have distinct windows in the fragmentation time and voltage in which the signal is maximized and produces spectra. While these experiments use a tickle voltage on the endcaps, other lab groups have worked with resonance ejection, where a resonant AC voltage is applied to one of the endcaps to achieve CID [23]. Such an AC voltage can yield significant increases in mass resolution, but greatly complicates the electronics needed to miniaturize.

As previously mentioned, fabricating a large array of micro-scaled cylindrical ion traps has the potential to significantly increase signal strength, showing the most promise for the development of a ruggedized, field-deployable instrument. Alignment is the biggest hurdle to overcome in the fabrications of CIT arrays. It is possible that multichannel detector and algorithm could be used to alleviate this problem. Next to alignment, the quality of the trap walls is also of concern; imperfections can cause aberrations in the field lines, which can be detrimental to the operation of the traps. SOI DRIE has become a method of choice for fabricating micrometer-scale devices while minimizing surface defects [24,25]. This process, and others like it, will be key in future instrumental development.

4. Conclusion

In this work, selective ion isolation and collision-induced dissociation were demonstrated using a 0.5 mm r_o ion trap that can be mounted and operated in a small package. CID parameters were explored and their effects on ion attenuation monitored in order to determine the optimum conditions under which to operate the mass spec. The scale of this instrument lends itself to portability, and with the ability to perform tandem mass spectrometry, it opens up a wide range of options for field use, even with reduced performance compared to its bench-top counterpart. With continued work to integrate small electronics, solid-state vacuum components (chemical getter pumps) and wireless capabilities, this device has the potential to fulfill the need for a rugged, field-deployable mass spectrometer. Such a device can be customized for use in environmental and water quality monitoring, first response and defense applications.

Acknowledgments

We would like to acknowledge First Detect (Grant No. G70710), Bill Whitten and Oak Ridge National Laboratories, and the University of North Texas Faculty Research Grant.

References

[1] E.R. Badman, R.G. Cooks, J. Mass Spectrom. 35 (2000) 659–671.
[2] C.R. Arkin, T.P. Griffin, J.A. Diaz, D.W. Follistein, C.H. Curley, D.P. Floyd, G.R. Naylor, W.D. Haskell, M. Blalock, F.W. Adams, Trac-Trend Anal. Chem. 23 (2004) 322–330.
[3] H.W. Chen, R.F. Xu, H. Chen, R.G. Cooks, Z. Ouyang, J. Mass Spectrom. 40 (2005) 1403–1411.
[4] I. Cotte-Rodriguez, E. Handberg, R.J. Noll, D.P.A. Kilgour, R.G. Cooks, Analyst 130 (2005) 679–686.
[5] J. Moxom, P.T.A. Reilly, W.B. Whitten, M. Ramsey, Anal. Chem. 75 (2003) 3739–3743.
[6] L. Gao, Q.Y. Song, G.E. Patterson, R.G. Cooks, Z. Ouyang, Anal. Chem. 78 (2006) 5994–6002.
[7] S.A. Lammert, A.A. Rockwood, M. Wang, M.L. Lee, E.D. Lee, S.E. Tolley, J.R. Oliphant, J.L. Jones, R.W. Waite, J. Am. Soc. Mass Spectrom. 17 (2006) 916–922.
[8] J. Fox, R. Saini, K. Tsui, G. Verbeck, Rev. Sci. Instrum. 80 (2009).
[9] W.B. Brinckerhoff, T.J. Cornish, R.W. McEntire, A.F. Cheng, R.C. Benson, Acta Astronaut. 52 (2003) 397–404.
[10] P.H. Dawson, Quadrupole Mass Spectrometry and its Applications, 2nd ed., American Institute of Physics, New York, 1995.
[11] M.N. Benilan, C. Audoin, Int. J. Mass Spectrom. 7 (1973) 421–432.
[12] S. Pau, C.S. Pai, Y.L. Low, J. Moxom, P.T.A. Reilly, W.B. Whitten, J.M. Ramsey, Phys. Rev. Lett. 96 (2006).
[13] E.R. Badman, R.G. Cooks, Anal. Chem. 72 (2000) 3291–3297.
[14] D. Cruz, J.P. Chang, M. Fico, A.J. Guymon, D.E. Austin, M.G. Blain, Rev. Sci. Instrum. 78 (2007).
[15] A. Chaudhary, F.H.W. van Amerom, R.T. Short, J. Microelectromech. Syst. 18 (2009) 442–448.
[16] F.H.W. Van Amerom, A. Chaudhary, M. Cardenas, J. Bumgarner, R.T. Short, Chem. Eng. Commun. 195 (2008) 98–114.
[17] J. Moxom, P.T.A. Reilly, W.B. Whitten, J.M. Ramsey, Rapid Commun. Mass Spectrom. 18 (2004) 721–723.
[18] W. Gohl, R. Kutscher, H.J. Laue, H. Wollnik, Int. J. Mass Spectrom. Ion Phys. 14 (1983) 411.
[19] B.A. Mamyrin, V.I. Karatev, D.V. Shmikk, V.A. Zagulin, Soviet Phys. JETP 37 (1973) 45.
[20] R.J. Cotter, C. Fancher, T.J. Cornish, J. Mass Spectrom. 34 (1999) 1368–1372.
[21] E.R. Badman, R.G. Cooks, Anal. Chem. 72 (2000) 5079–5086.
[22] E. Sokol, K.E. Edwards, K. Qian, R.G. Cooks, Analyst 133 (2008) 1064–1071.
[23] J. Moxom, P.T.A. Reilly, W.B. Whitten, J.M. Ramsey, Rapid Commun. Mass Spectrom. 16 (2002) 755–760.
[24] R. Abdolvand, F. Ayazi, Sens. Actuators A: Phys. 144 (2008) 109–116.
[25] S.S. Yun, D.H. Jeong, S.M. Wang, C.H. Je, M.L. Lee, G. Hwang, C.A. Choi, J.H. Lee, J. Micromech. Microeng. 19 (2009).